Published in final edited form as:
Brain Behav Immun. 2013 May ; 30: 33–44. doi:10.1016/j.bbi.2012.09.010.

Absence of CCL2 is sufficient to restore hippocampal neurogenesis following cranial irradiation

Star W. Lee[1], **Ursula Haditsch**[1], **Branden J. Cord**[1], **Raphael Guzman**[1,2], **Soo Jeong Kim**[1], **Chotima Boettcher**[3], **Josef Priller**[3], **Brandi K. Ormerod**[4], and **Theo D. Palmer**[1,*]

[1]Stanford University, Institute for Stem Cell Biology and Regenerative Medicine, Stanford, CA [2]Department of Biomedicine, University of Basel, Basel, Switzerland [3]Neuropsychiatry and Laboratory of Molecular Psychiatry, Charite-Universitaetsmedizin, Berlin, Germany [4]J. Crayton Pruitt Family Department of Biomedical Engineering, University of Florida, Gainesville, FL

Abstract

Cranial irradiation for the treatment of brain tumors causes a delayed and progressive cognitive decline that is pronounced in young patients. Dysregulation of neural stem and progenitor cells is thought to contribute to these effects by altering early childhood brain development. Earlier work has shown that irradiation creates a chronic neuroinflammatory state that severely and selectively impairs postnatal and adult neurogenesis. Here we show that irradiation induces a transient non-classical cytokine response with selective upregulation of CCL2/monocyte chemoattractant protein–1(MCP-1). Absence of CCL2 signaling in the hours after irradiation is alone sufficient to attenuate chronic microglia activation and allow the recovery of neurogenesis in the weeks following irradiation. This identifies CCL2 signaling as a potential clinical target for moderating the long-term defects in neural stem cell function following cranial radiation in children.

Keywords

CCL2/MCP1; radiation; neurogenesis; inflammation; hippocampus

1. INTRODUCTION

Radiation therapy is used in the treatment of many cancers and when the radiation fields include the central nervous system (CNS), patients often experience delayed and progressive neurological sequelae (Abayomi, 1996; Madsen et al., 2003). This is particularly true of very young patients and is pronounced when the irradiation fields encompass the late-developing structures of the brain that support ongoing neurogenesis, such as the temporal lobe and ventricular zones. Hippocampus- dependent functions of learning and memory are exquisitely sensitive to radiation therapy in both children and animals (Abayomi, 1996; Madsen et al., 2003; Mizumatsu et al., 2003; Saxe et al., 2006). In rodents, it has been shown that neurogenesis within the granule cell layer of the hippocampal dentate gyrus is a

*To whom correspondence should be addressed: tpalmer@stanford.edu, The Lorry I. Lokey Stem Cell Research Building, 265 Campus Dr., Stanford, CA 94305-5454, 650-736-1482 phone, 650-736-1949 fax.

strong predictor of hippocampal functional integrity (Shors et al., 2001; Shors et al., 2002) and it is now known that even a single fraction of irradiation can permanently ablate >90% of postnatal hippocampal neurogenesis in rodents (Monje et al., 2002).

It is thought that radiation therapy reduces postnatal neurogenesis through two mechanisms. Ionizing radiation induces an acute apoptosis in dividing progenitor cells thereby reducing the pool of mitotic neural stem and progenitor cells (Limoli et al., 2004; Mizumatsu et al., 2003). Radiation-induced changes to signaling within the progenitor cell microenvironment further reduces the fraction of remaining cells that adopt a neuronal fates and integrate into the adult hippocampal neural network (Ekdahl et al., 2003; Monje and Palmer, 2003). Combined, these two effects can virtually eliminate neurogenesis in adult rats following a single exposure to 10 Gy cranial X-irradiation. In humans, multiple fractions are used and we have shown in post-mortem analysis that neurogenesis is impaired in the hippocampus for up to 15 years following radiotherapy (Monje et al., 2007).

Microglial recruitment and activation plays a significant role in this injury response and we have found that the extent of microglial activation inversely correlates with post-irradiation neurogenesis (Monje and Palmer, 2003). Modification of the inflammatory state with non-steroidal anti-inflammatory drugs (NSAIDS) can partially restore neurogenesis in the irradiated rodent hippocampus (Monje et al., 2002; Monje et al., 2003) suggesting that innate immune activation and chronic inflammation plays an important role in neural progenitor regulation. Although steroidal anti-inflammatory drugs are often used following cranial irradiation, these drugs can directly inhibit neurogenesis (Cameron et al., 1998; Gould et al., 1992) and novel strategies for controlling inflammation are needed if protecting postnatal neurogenesis is to be included in clinical treatment goals. Unfortunately, the specific immune signaling cascades that mediate this unusually persistent inflammation are unknown and targeted anti-inflammatory strategies do not yet exist.

In vitro and *in vivo* models of hippocampal neurogenesis have shown that activation of the innate proinflammatory response inhibits neurogenesis through both cytokine-mediated inhibition of neuronal differentiation as well as reduced newborn cell survival (Ekdahl et al., 2003; Mizumatsu et al., 2003; Monje and Palmer, 2003). Non-steroidal anti-inflammatory drugs (NSAIDs) can attenuate these effects and one of the most robust effects of NSAID treatment in the context of irradiation injury is a reduction of microglia/monocyte recruitment and activation (Monje et al., 2003), suggesting monocyte pro-inflammatory signaling may contribute to the persistence of microglial activation.

Our earlier work suggested that CD45-expressing macrophages recruited to the brain from the periphery may specifically contribute to the deficits and that monocyte-specific interventions may be useful in combating the delayed effects of cancer therapies (Monje et al., 2003). In addition, we show here that the acute cytokine response following cranial irradiation in mice implicates several inflammatory chemokines known for their role in the recruitment and extravasation of monocytes following injury (Fig. 1). Notable among these is the chemokine CCL2/MCP-1, a CC-family chemoattractant cytokine (Matsushima et al., 1989) that is intrinsically involved in the early activation and recruitment of monocytes to areas of tissue injury such as those caused by atherosclerosis, arthritis, and stroke (Chen et al., 2003; Gu et al., 1998; Ogata et al., 1997). Interestingly, increased systemic levels of CCL2 observed during aging have recently been associated with decreased neurogenesis and age-related cognitive impairments, suggesting that blood-borne chemokines such as CCL2, CCL11 and CCL12 are potentially critical contributors to the susceptibility of the ageing brain to cognitive impairments (Villeda et al., 2011).

Within the CNS, CCL2 production by astrocytes, microglia, and endothelial cells is stimulated via NF-κB signaling in response to the immediate-early pro-inflammatory cytokines IL-1β, INF-γ or TNF-α (Hayashi et al., 1995; Luo et al., 1994; Thibeault et al., 2001). Originally identified as a tumor-derived chemotactic factor, CCL2 is also known to inhibit tumor growth, presumably by nonspecific recruitment of monocytes to the tumor site (Bottazzi et al., 1992).

CCL2 acts through its receptor CCR2 to activate the p42/44 MAP kinase cascade, leading to upregulation of surface adhesion molecules on circulating and tissue-resident immune cells. CCL2 also causes endothelium to upregulate cognate adhesion molecules leading to leukocyte adhesion and extravasation. CCL2 is also known to stimulate the release of primary proinflammatory cytokines such as TNFα and IL-1β from a variety of immune cells (Biswas and Sodhi, 2002; Ferreira et al., 2005).

Mice lacking the CCL2 receptor CCR2 show reduced secretion of acute innate Th1 pro-inflammatory cytokines, such as IFN-γ and reduced leukocyte extravasation to sites of tissue injury (Traynor et al., 2002). In addition to its acute proinflammatory effects, CCL2 also acts later in the immunological cascade to promote Th2 immuno-modulatory release of IL-4, an anti-inflammatory cytokine (Gu et al., 2000), suggesting roles in both acute innate proinflammatory response as well as in modulation of the subsequent adaptive immune response. IL-4 is also implicated in pro-neurogenic signaling that promotes neurogenesis (Butovsky et al., 2006) and it is possible that MCP-1 may play both anti-neurogenic and pro-neurogenic roles in the irradiation injury model.

Here we examine the role of CCL2/MCP-1 in post-irradiation neuroinflammation and stem cell dysfunction within the mouse hippocampus. By examining markers of chronic inflammation, macrophage extravasation and evaluating the disruption of hippocampal neurogenesis in irradiated young adult mice, we show here that the absence of CCL2 is alone sufficient to allow the neurogenic microenvironment of the adult hippocampus to normalize within 4 weeks of irradiation. Paradoxically, expression of CCL2 is only detected in the first hours after irradiation yet loss of this single chemokine is sufficient to allow neurogenesis to recover in this model. The combined data indicates that the immunological response to radiation injury involves a unique profile of pro-inflammatory cytokines and that these cytokines highlight the importance of monocyte/microglial-selective activation in the chronic inhibition of adult neurogenesis following radiation therapy.

2. METHODS

2.1 Cranial irradiation

$CCL2^{-/-}$ animals were kindly provided by B. J. Rollins (Ferreira et al., 2005) and E. Mocarski. Age matched congenic WT (WT) control BALB/c mice were purchased from Jackson Laboratories. 2–3 month old adult male mice were anesthetized with ketamine and xylazine and exposed to cranial irradiation using a Philips orthovoltage X-ray system operated at 200 kVp and 20mA. On Day 0, a single dose of 10 Gy was limited by lead shielding to a 1-cm diameter column that included left and right hippocampal formations. The remaining body, neck, eyes, ears and snout were shielded from irradiation. Dosimetry and field dimensions were confirmed using TLD dosimeters (K & S Associates, Nashville, Tennessee) buried in the hippocampi and surrounding brain areas of euthanized mice. The dose rate was approximately 89.0 cGy/minute. Non-irradiated controls for all experiments received anesthesia only.

2.2 BrdU injections and tissue preparation

Animals were injected intraperitoneally with BrdU once per day for 6 days on days 1–6, 15–20, or 28–33 after irradiation (50 mg/kg per day using a 10 mg / ml solution in saline, Sigma, prepared fresh on the day of injection). Animals were anesthetized and sacrificed 1 week (1wk), 1 month (1mo) or two months (2mo) after irradiation (see Fig. 2). Brains were fixed by transcardial perfusion with 4% paraformaldehyde (PFA), removed from the skull and postfixed overnight in 4% PFA, and then equilibrated in phosphate buffered 30% sucrose. Free floating 40 μm sections were collected on a freezing sledge microtome and stored in tissue cryoprotectant solution at −20°C until used.

2.3 Immunohistochemistry

Free floating sections were immunostained as previously described in (Monje et al., 2003; Palmer et al., 2000) using the following primary antibodies and working concentrations: mouse anti-NeuN monoclonal antibody (1:500, Chemicon, Temecula, California); goat anti-doublecortin (1:500, Santa Cruz Biotechnology, Santa Cruz, California); rabbit anti-Iba1 (1:1500, Wako, New Jersey); rat anti-BrdU (1:500, Accurate Chemical, Westbury, New York); rat anti-CD68 (Fa-11; 1:40, Serotec, Raleigh, North Carolina); guinea pig anti-GFAP (1:750, Advanced Immunochemicals, California); mouse anti-APC (1:100, Calbiochem, San Diego, California), biotinylated tomato lectin (*Lycopersicon esculentum*) (1:200, Vector Laboratories, Burlingame, California). Fluorochrome conjugated, minimally cross-reactive secondary antibodies produced in donkeys to recognize the appropriate primary antibody species and isotype controls were purchased from Jackson ImmunoResearch (West Grove, Pennsylvania). Primary and secondary antibody binding was allowed to reach equilibrium overnight at 4°C. Sections were washed with saline and post-fixed with 4% PFA for 10 min at room temperature. Sections were then mounted on glass slides for evaluation. For animals injected with Combidex®, iron detection was achieved using a standard Prussian blue reaction (2% hydrochloric acid and 2% potassium-ferricyanide in distilled water).

2.4 Luminex assay

Preconfigured kits are purchased from Panomics/Affymetrix and assay is performed according to Manufactures recommendation with few modifications: Briefly: Samples in duplicates (25μl) are added to a 96 well filter plate containing Assay buffer. Standards (7 point dilutions) and controls are added and then the appropriate plexus of Antibody linked to polystyrene beads is added at this time. Samples are incubated for 2 hours at room temperature while shaking at a constant speed (500rpm). Incubation is continued overnight at 4°C without shaking. Wells are then washed 2X to remove unbound antigen sample. Biotinylated antibody for detection of the different antibodies is then added to the bead mixture in each well (25μl) and incubated for 2 hours with shaking at room temperature as above. The mixture is vacuum aspirated and washed 2X to remove excess detector antibody. SA-PE (50μl) is added to the mixture and incubated for 30 minutes with shaking at room temperature. The mixture is vacuum aspirated, washed 2X, and re-suspended in 120ul Reading buffer and incubated for 3 minutes at room temperature with shaking. The 96 well plate is transferred to the Luminex reader for quantitative analysis. Individual cytokines/chemokines are identified and classified by their bead color using the Red laser and cytokine levels are quantified using the Green laser. Digital images of the bead array are captured following laser excitation using a Pixel CCD camera and are processed on a computer workstation. Standard curves and report of the unknown cytokine levels in the samples are prepared using BeadView and MiraiBio software.

2.5 ELISA

To isolate protein from the brain, animals were first perfused with ice cold saline. The brains were removed and placed in protein lysis buffer consisting of 1% Triton-X 100, 0.5% NP-40, 25mM Tris HCL, 100mM NaCl, and protease inhibitors (1:100). For CCL2 quantification, on day 1, a 96-well plate (Costar) was coated overnight at 4°C with a capture antibody of 2μg/mL (BD Pharmingen, San Diego, California) in 0.1M sodium carbonate. On day 2, the plate was washed twice with wash buffer (PBS/0.05% Tween) and then blocked in PBS/3%BSA for 2h at room temperature. Tissue samples and standards were incubated overnight at 4°C. On Day 3, the plate was washed four times with wash buffer and then loaded with 1ug/mL biotinylated antibody for 45min at room temperature. The plate was then washed six times, loaded with 5ug/mL avidin-HRP (Sigma) for 30min at room temperature, and washed again. The ELISA was developed using 3,3′,5,5′-tetramethylbenzidine (Sigma) in phosphate citrate buffer. The plate was read at 650nM using an ELISA microplate reader (Molecular Devices, Sunnyvale, CA).

2.6 Confocal microscopy and image processing

All confocal microscopy was performed using a Zeiss LSM 510 Meta confocal microscope. Appropriate gain and black level settings were determined on control tissues stained with secondary antibodies alone. Upper and lower thresholds were set using the range indicator function to minimize data loss through under or over saturation. Images were subsequently exported as TIFF files and post-processed using Adobe CS2 software for figure production.

2.7 Cell quantification and unbiased stereology

All counts were limited to the hippocampal granule cell layer proper and a 50μm border along the hilar margin that included the neurogenic subgranular zone. The proportion of BrdU cells displaying a lineage-specific phenotype was determined by scoring the co-localization of cell phenotype markers with BrdU using confocal microscopy. Split panel and z-axis orthogonal projections were used for all counting to minimize false positives. All counts were performed using multi-track configurations with a 40× objective and electronic zoom of 2. When possible, 100 or more BrdU-positive cells were scored for each marker per animal. Each BrdU-positive cell was manually examined in its full “z”-dimension and only those cells for which the nucleus was unambiguously associated with the lineage-specific marker were scored as positive. The total number of BrdU-labeled cells per hippocampal granule cell layer and subgranular zone was determined using immuno-detection of BrdU followed by HRP-coupled secondary antibodies and diaminobenzadine stain (Vector Laboratories). Stained BrdU-positive nuclei were scored under light microscopy using Microbrightfield Stereo Investigator software and a modification of the di-sector method where random grid placement provided systematic and unbiased sampling of BrdU cell density within the dentate gyrus. Nuclei at both cut surfaces were scored and over estimation was corrected using the Abercrombie method for nuclei with empirically determined average diameter of 13 μm within a 40 μm section. All analyses were performed by investigators blinded to sample identity and treatment group.

2.8 Pixel intensity and staining density analysis

Tissue sections from each animal were stained in a single staining run to ensure that each section was processed under identical immuno-staining conditions. Low magnification images of the dentate gyrus were collected on the confocal microscope with a 10× objective using care to define gain and contrast settings that ensured all pixels within any given section fell within the photomultiplier detection range (e.g., settings that ensured no under saturated or over saturated pixels in any tissue section). Images were then collected from all tissue sections in a single acquisition session without altering confocal settings. Photoshop

CS3 or NIH ImageJ was used to evaluate pixel intensity as follows. In each image, the dentate gyrus and subgranular zone were outlined and the total number of pixels within the outlined region was recorded. Pixels positive above background for a given marker were subsequently selected and the number of positive pixels within the outlined region of interest also recorded to determine the % of the dentate area occupied by positive staining. Average pixel intensity for all positive pixels was recorded to document relative intensity of staining for a given epitope. Unlike enzyme linked detection systems that deposit insoluble substrates to an opaque endpoint, fluorescent immunological detection reactions that are allowed to reach equilibrium will produce fluorescent signals that are proportional to the abundance of the detected epitope.

2.9 Progenitor cell culture and differentiation

Whole brains from P0 mouse pups were enzymatically digested with a mixture of papain, neutral protease, and DNase. Neurospheres were cultured on uncoated plates with medium containing Neurobasal (Gibco), L-glutamine, PSF, B-27 without vitamin A, 20ng/ml FGF-2, and 20ng/ml EGF. Cultures were passaged in parallel when reaching confluence. Cells were induced to differentiate by plating dissociated cells into laminin-coated multi-chamber tissue culture slides (Nunc) in differentiation media, Neurobasal, B-27 without vitamin A, 1% fetal bovine serum, 100 nM all trans-retinoic acid, 1 ng/ml FGF-2, 10ng/ml BDNF, and 10ng/ml NT3. Recombinant murine monocyte chemoattractant protein-1 (rmMCP-1; 0–100nM; Peprotech, Rocky Hill, New Jersey) was added to some wells and cells allowed to differentiate for 5 or 14 days. During this period, cells were fed every other day with fresh media supplemented with rmMCP-1. Cells were then fixed with 2% PFA and stained. Confocal photomicrographs (40× zoom of 1) were taken at systematically sampled intervals along a diagonal path through each well, collecting 5 fields per well. Total nuclei per sample site was scored using DAPI, neurons were scored on the basis of doublecortin (Dcx) immunoreactivity.

2.10 Flow cytometry

Mice were anesthetized with ketamine and xylazine. Brains were removed and rinsed with PBS. Whole brain tissues were then enzymatically dissociated using a mixture of papain (Worthington, Lakewood, New Jersey), neutral protease dispase II (Roche, Indianapolis, Indiana), and DNase (Worthington) as previously described (Gage et al., 1998). After 1 hour dissociation at 37°C, single cell suspensions were fractionated over two sequential Percoll gradients and a monocyte-enriched fraction was collected consisting of cells that initially sedimented in 25% Percoll and then floated in 70% Percoll. Cells were washed twice in media consisting of DMEM/F12 and 10% heat inactivated FCS. Cells were chilled to 4°C and stained live using FITC-anti mouse CD45 (1:500) and PE-anti mouse CD11b (1:500) (BD Pharmingen, San Diego, California) for 10 min at 4 °C. Subsequently, cells were washed 3 times in PBS and fixed with 2% Paraformaldehyde for 5 minutes. Becton Dickinson FACScan and CELLQuest software were used for cell analysis and data acquisition. FlowJo software was used for post-acquisition analysis.

2.11 eGFP-positive bone marrow chimeras

Bone marrow transplant was performed essentially as previously described (Priller et al., 2001). Prior to bone marrow transplantation, recipient mice received either 11 Gy total body irradiation (including head) or 11 Gy body-only irradiation (head-protected with 6cm thick lead shield). Whole bone marrow cells (BMCs) were collected from 8–12 week-old EGFP-transgenic mice (Okabe et al., 1997) and 5×10^6 total BMCs were transplanted to irradiated hosts by tail vein injection. 4 weeks after bone marrow transplantation, engraftment was confirmed by analyzing peripheral blood cells for GFP-expression by FACS and brains were

collected from reconstituted animals for histological evaluation of GFP-positive cells within the irradiated or non-irradiated brain.

2.12 Combidex labeling of peripheral macrophages

Peripheral monocyte phagocytosis of ultra small iron particles can be used to label circulating macrophages *in vivo* and was used here as a method to determine if peripheral macrophages were recruited into the irradiated brain during the acute injury phase following irradiation. WT and CCL2$^{-/-}$ animals were irradiated with a single 10 Gy cranial dose that was restricted to one hemisphere with lead shielding. On day 4 after irradiation, animals were injected intravenously with a single bolus of dextran-coated ultra small super-paramagnetic iron oxide particles (USPIO, Combidex, 1 mg/kg in saline), which are rapidly phagocytized by circulating monocytes (Weissleder et al., 1990). Brains were subsequently harvested on day 7 and evaluated histologically with Prussian blue staining for iron-loaded macrophages.

2.13 Middle cerebral artery occlusion (MCAO)

As a positive control for the ability to detect peripheral macrophage recruitment, Sprague-Dawley rats (Charles River, Wilmington, MA) were evaluated following an experimental focal cerebral ischemic event. Male animals weighing 280–320 g were anesthetized with 2.5% isoflurane in an oxygen/air mixture. Temperature, EKG and respiration rate were monitored throughout the surgery. The common carotid (CCA), external carotid and pterygopalatine arteries were exposed and ligated on the left side. The left internal carotid artery (ICA) was transiently occluded with a microsurgical clip, and an arteriotomy was made in the CCA. A 3.0-monofilament suture (Ethicon, Sommerville, NJ) with a rounded tip was inserted into the CCA and advanced through the ICA to the ostium of the middle cerebral artery (MCA) to occlude the MCA (MCAO). The suture was left in place for 2 hours, and then removed to allow reperfusion. Intravenous Combidex injections were administered 3 days after MCAO and brains evaluated 4 days later (1 wk after MCAO).

2.14 Statistics

All experiments were analyzed using ANOVA, unless otherwise indicated. Newman-Keuls or Bonferroni tests were used for posthoc analysis.

3. RESULTS

3.1 Transient expression of monocyte chemoattractants accompanies microglial activation following cranial irradiation

Young adult BalbC mice were treated with a single exposure to 10 Gy cranial irradiation in a 1cm vertical column centered over the hippocampus (Fig. 1A, B). One week later, brains were collected and immunostained for Iba1 to identify all monocyte/microglia lineage cells and co-stained for CD68 to evaluate monocyte activation within the neurogenic zone on the hippocampal granule cell layer (GCL) (Fig. 1D–F). CD68 is a lysosome-associated epitope that is upregulated in activated macrophages and microglia (Imai et al., 1996; Ramprasad et al., 1996). One week following irradiation, the density of microglia in the irradiated hippocampus was not different than in irradiated wild-type animals (not shown). In both genotypes, there was a notable increase in microglial activation illustrated by CD68 immunoreactivity (Fig. 1E, F).

To determine the cytokine profiles that accompanied the radiation-induced microglial activation, hippocampal formations were collected from non-irradiated controls and from irradiated animals at 6 and 24, hrs after irradiation. Tissue extracts were evaluated by Luminex multiplex assays for 23 cytokines and chemokines (Supplemental Table 1). Of

these, only 4 cytokines or chemokines were elevated above baseline following irradiation; IL-12 p40, KC, CCL2 and CCL7 (Fig. 1G). Of these, CCL2 was by far the most abundant radiation-induced cytokine or chemokine. ELISA was used to confirm the CCL2 response at 3, 6, 9, 12, 24, 48 hrs, 7 days and 1 month following irradiation. ELISA confirmed a similar short time course of CCL2 expression, which peaked by 6 hrs and returned to baseline within 24 hrs (Fig. 1H). CCL2 was not detectably elevated at one week or one month following irradiation, suggesting that CCL2 is primarily active in the acute stages of the injury response.

3.2 CCL2 does not act through the recruitment of peripheral monocytes to sites of irradiation injury

In our earlier work (Monje et al., 2003), we noted that a subpopulation of CD11b positive microglia were decorated by the marker NG2 a phenotype previously attributed to peripheral blood monocytes after irradiation (Bu et al., 2001; Jones et al., 2002) and we speculated that invading peripheral macrophages were required for the anti-neurogenic neuroinflammatory state following irradiation. The rapid spike in CCL2 is consistent with peripheral monocyte recruitment in response to radiation injury and suggested that the absence of CCL2 might prevent macrophage extravasation and moderate the immune impact on neurogenesis.

To examine the role that CCL2 might play in the acute recruitment of peripheral monocytes in response to irradiation, wild type BalbC mice and BalbC mice null for the CCL2 protein ($CCL2^{-/-}$) (Lu et al., 1998; Muessel et al., 2002) were irradiated. Brains were harvested one week after 10 Gy irradiation and enzymatically dissociated into single cells. Percoll gradients were used to enrich for leucocytes and eliminate mature neurons, glia, and myelinated neuropil. The remaining cells were stained for CD45 or CD11b to identify all immune cells or monocytes, respectively. Prior reports have shown that peripheral macrophages can be distinguished from resident microglia by elevated CD45 expression (Ford et al., 1995; Pais and Chatterjee, 2005). Flow cytometric analysis of cells isolated from irradiated WT or $CCL2^{-/-}$ animals showed that there were very few cells with elevated CD45 expression and there was no detectable difference in the proportion of CD45 low vs. high monocytes following irradiation in either genotype (Fig. 2A, B).

We also evaluated monocyte recruitment using a second method involving the peripheral labeling of circulating monocytes by intravenous dextran-coated ultra small super-paramagnetic iron oxide particles (USPIO, Combidex) following irradiation. Animals were irradiated and then injected on day 4 with Combidex (1 mg/kg in saline via the tail vein). On day 7, brains were collected and evaluated for iron containing cells via Prussian blue staining (Fig. 2C, D). There were extremely low numbers of iron containing macrophages within the hippocampus one week after irradiation and no measurable difference between $CCL2^{-/-}$ and WT animals. In contrast, a more aggressive injury caused by focal ischemia did recruit a significant number of monocytes into the injured areas of the brain (Fig. 2E), showing that the method can detect extravasation of peripheral cells, yet very few Prussian blue-positive macrophages were found within the irradiated brains.

Finally, to determine whether low levels of peripheral lymphocyte recruitment over time might ultimately lead to elevated peripheral macrophage numbers in the irradiated hippocampus, recipient mice received either 11 Gy total body (including head) irradiation or 11 Gy body-only irradiation (head-protected with 6cm thick lead shield) and then injected with bone marrow obtained from 8–12 week-old EGFP-transgenic mice (Okabe et al., 1997). 4 weeks after bone marrow transplantation, peripheral engraftment was confirmed by analyzing peripheral blood cells for GFP-expression by FACS and brains from animals showing significant GFP-chimerism were evaluated for the presence of GFP-positive cells within the irradiated or non-irradiated brain. Extremely few GFP-positive cells were noted in

any of the engrafted animals (less than 5 per entire hippocampal formation, Fig. 2F). This confirms earlier studies reporting that irradiation recruits very low numbers of myeloid cells to the hippocampus (Mildner et al., 2007; Priller et al., 2001; Turbic et al., 2011), and suggests that a chronic increase in infiltrating bone marrow-derived cells are unlikely to play a significant role in the chronic inflammatory signaling that mediates the neurogenic defects in the hippocampus after irradiation.

3.3 Absence of CCL2 allows neurogenesis to recover

To determine whether absence of CCL2 signaling would be protective, wild type $CCL2^{-/-}$ mice were irradiated and then injected with BrdU at different times following irradiation to evaluate neurogenesis. Brains were collected 1, 4 and 8 weeks after irradiation and hippocampal neurogenesis evaluated by immunofluorescent and immunohistochemical staining (Fig. 3). To evaluate neurogenesis in the week following irradiation (during the acute phase of the injury response), animals were injected with BrdU once each day for 6 days (50mg/kg, IP) and sacrificed on day 7 (Fig. 3C). To evaluate neurogenesis during the sub-acute phase of the injury response, BrdU injections were given on days 15–20 and animals were then sacrificed on day 28, one month after irradiation. To evaluate neurogenesis in the chronic phase of the irradiation injury response animals were given 6 daily BrdU injections starting from day 28 and allowed to survive an additional 3 weeks and then sacrificed at two months after irradiation.

Tissues were immunostained for BrdU to detect newborn cells and counter-stained for doublecortin (Dcx, immature neurons), and NeuN (mature neurons) (Fig. 3A, B). The total number of BrdU cells per hippocampus was determined using unbiased stereological methods (Fig. 3D). The fraction of those BrdU-labeled cells expressing neuronal markers was also determined by confocal analysis (Fig. 3E). In both wild type and $CCL2^{-/-}$ irradiated mice, the abundance of new $BrdU^{+}$ cells was significantly reduced at all time points after irradiation indicating that the absence of CCL2 did not prevent the loss of neural progenitor cells after irradiation, nor did absence of CCL2 promote repopulation of the neurogenic niche. However, for those proliferative cells that remained at 1 month following irradiation, the absence of CCL2 allowed full recovery of neuronal differentiation and survival with no significant difference in the fraction of cells adopting a neuronal fate between control and irradiated CCL2-deficient mice.

To evaluate the chronic activation state of the resident microglia in wild type and $CCL2^{-/-}$ animals, tissues were collected 2 months after irradiation (using the BrdU paradigm shown in Fig. 3E) and then immunostained for BrdU, Iba1 (total microglia), and CD68 (Fa-11, activated microglia) (Fig. 4). Overall microglial density and arborization in the hippocampal dentate gyrus was evaluated by measuring Iba1-positive pixels within the dentate granule cell layer and subgranular zone (Fig. 4A, B, F and Supplemental Fig. 1). Microglial staining was present at similar densities in WT and $CCL2^{-/-}$ control animals and irradiation did not significantly increase Iba1 staining density in either WT or $CCL2^{-/-}$ animals (Fig. 4F), suggesting that the total microglial burden was not different in either genotype following irradiation.

The fraction of BrdU-positive cells co-labeled for Iba1 was determined by confocal microscopy (Fig. 4C, G). Few of the BrdU-positive cells in non-irradiated wild-type or $CCL2^{-/-}$ animals were positive for microglial markers indicating a low level of microglial proliferation in the absence of injury. Irradiation increased this number from 4 ± 1% (n=9) in WT controls to 31 ± 6% ($p<0.001$, n=9) in irradiated WT animals (Fig. 4G), indicating a dramatic proliferative recruitment of microglia that persists for at least 28 days following irradiation in wild type animals. In contrast, the absence of CCL2 allowed the post-injury proliferative response to normalize to levels similar to non-irradiated controls at this same

time point (1 month following irradiation). Similarly, evaluation of activation status by CD68 staining showed that staining intensity associated with microglia was elevated by 1.8 fold ($p<0.05$) in WT animals following radiation but was not significantly elevated in $CCL2^{-/-}$ animals ($p>0.05$, n=5) (Fig. 4H). As seen in human subjects (Monje et al., 2007), persistent CD68 expression in the mouse indicates that radiation is accompanied by a chronic microglial activation and low grade proliferative response. The absence of CCL2 allowed this activation/proliferation to resolve by one month following irradiation.

3.4 Absence of CCL2 speeds neurogenic recovery by restoring newborn neuron maturation

To more closely evaluate the defects in neurogenesis and recovery in $CCL2^{-/-}$ mice, total newborn cells in the dentate gyrus were quantified by unbiased stereology and categorized based on expression of markers for immature vs. mature neurons. Neural progenitor cells within the hippocampus initially produce immature neuroblasts that are characterized by a migratory phenotype and expression of Dcx (Francis et al., 1999). As newly generated neuroblasts mature, they arborize, establish synaptic connections and eventually establish patterns of neuronal activity that are indistinguishable from the surrounding preexisting neurons (Filippov et al., 2003; Kronenberg et al., 2005; van Praag et al., 2002). During this process, NeuN expression is upregulated and Dcx is down regulated as the cells become postmitotic. Newborn neurons eventually lose Dcx expression as they become mature (Filippov et al., 2003; Kronenberg et al., 2005).

To evaluate the effects of irradiation on neuronal maturation, newborn neurons were divided into three categories, immature neurons (Dcx-alone), transition state neurons (Dcx + NeuN), or mature neurons (NeuN-alone, as illustrated in Fig. 2A,B). Unbiased stereology was used to document the total number of BrdU-labeled cells and then this number was multiplied by the fraction of BrdU+ cells that expressed each marker to produce the total newborn cell number per hippocampus. At the 1 wk time point, animals were sacrificed immediately after BrdU-injections and, as expected, most newborn neurons within the control hippocampus were still immature (positive for only Dcx) (Fig. 5A). Irradiation decreased the absolute number of immature neurons in wild type mice to approximately 20% of control levels (3088 ± 456 cells (n=3) vs. 618 ± 19 cells, $p<0.001$, n=3). Similar numbers of new neurons were generated in control $CCL2^{-/-}$ animals and irradiation similarly reduced the abundance of newborn neurons to approximately 18% of non-irradiated $CCL2^{-/-}$ mice (from 2695 ± 476 cells (n=3) to 786 ± 100 cells, $p<0.001$, n=4). Only a small number of BrdU positive cells expressed markers for transition state or mature neurons at this time point. There were no significant differences between wild type and CCL2−/− animals indicating that neurogenesis was equally impacted in both genotypes in the week following irradiation.

BrdU labeling on days 15–20 following irradiation and evaluation at day 28 (Fig. 5B) showed that the prior irradiation still significantly reduced the abundance of immature neurons in both wild type and $CCL2^{-/-}$ animals. Dcx-only cells decreased from 1585 ± 159 to 815 ± 142 in wild type animals ($p<0.001$, n=4) and from 1378 ± 198 (n=3) to 498 ± 93 cells in $CCL2^{-/-}$ animals ($p<0.001$, n=3). Dcx+NeuN double positive transition state neurons were also reduced from 803 ± 186 to 307 ± 187 cells in wild type animals ($p<0.05$) and from 993 ± 238 to 269 ± 98 cells in $CCL2^{-/-}$ animals ($p<0.001$). Few cells expressed NeuN-only at this time point, even in control wild type animals since the time delay between BrdU labeling and evaluation (one week) was too short to allow cells to fully mature. Again, there were no significant differences between wild type and $CCL2^{-/-}$ animals at this time point.

BrdU labeling at one month followed by evaluation at two months after irradiation revealed that transition-state and mature neurons were still significantly depleted in wild type animals

(Dcx+NeuN, 45 ± 3% of all BrdU-positive cells in non-irradiated controls vs. 14 ± 5% in irradiated WT animals, leading to an 83% loss in the total number of transition state neurons in WT irradiated animals, $p<0.001$). This loss was significantly attenuated in $CCL2^{-/-}$ animals (WT irradiated vs. CCL2 irradiated, $p < 0.05$, $n \geq 5$). In both WT and $CCL2^{-/-}$ animals, irradiation was accompanied by a 30–40% decrease in cells that expressed NeuN alone suggesting that the absence of CCL2 improved neuronal maturation at the early Dcx to NeuN transition where newborn cells initially establish their arborization but does not fully normalize the kinetics of the final maturation stage into NeuN-only neurons. The net result (i.e., the total number of newborn neurons in all maturation states) was 39 ± 2% of control levels in WT irradiated animals vs. 63 ± 9% of control levels in $CCL2^{-/-}$ animals, representing a significant overall protection of neurogenesis in the absence of CCL2 ($p < 0.05$, $n \geq 5$).

To determine if the alterations in neuronal maturation were mirrored by defects in neuron arborization, sections stained for Dcx were evaluated for the area of the dentate innervated by Dcx-positive arbors (Fig. 5D). The loss of Dcx/NeuN transition state neurons was accompanied by a dramatic decrease in total area of Dcx immunoreactivity within the granule cell layer of the hippocampus ($p < 0.05$). This loss was significantly attenuated in $CCL2^{-/-}$ animals (Fig. 5E).

4. DISCUSSION

Here we show that absence of CCL2 signaling after irradiation allows partial recovery of neurogenesis in the second month after irradiation.

Previous studies have shown that CCL2 expression peaks acutely within 6 hrs of irradiation (Kalm et al., 2009; Lee et al., 2010). We confirmed and extended these findings and show here that CCL2 expression remains low even 1 month after the irradiation (Fig. 1H). Given the fact that CCL2 expression returns to baseline within 24 hrs of irradiation, it seems unlikely that CCL2 itself mediates the slow recovery of neurogenesis. Instead it seems more likely that the influence of CCL2 on neurogenesis is mediated indirectly by either the amplitude or quality of the initial activation of microglia within the neurogenic niche that subsequently sets the stage for the persistence of microglial activation. In the absence of this acute CCL2-dependent signaling, the inflammatory state that inhibits neuronal maturation resolves more quickly. We did note that standard curves generated using Luminex internal controls generated lower estimates of protein abundance than those generated using the ELISA assays (this was true for most cytokines tested); however, the timing of CCL2 expression was identical for both assays.

Initially we speculated that peripheral macrophages may play a role in mediating the persistent negative effects (Monje et al., 2003), but our present studies suggest that only a very small fraction of monocytes in the brain are recruited from the periphery in the months following irradiation (Fig. 2). Instead, it appears that the chronic inflammatory state is mediated exclusively by the effects of radiation on resident microglia and/or other non-marrow derived cells of the brain. Although there is no apparent increase in the abundance of microglia in irradiated wild type animals, a significant fraction of the dividing cells in the hippocampus are microglia (~30%), suggesting that irradiation evokes both activation and rapid turn-over of microglia. The consistent size of the microglia population is likely due to cell death of microglia, which occurs after an increase in proliferation as previously reported in other injury models (Vela et al., 2002). This persistent proliferation of activated microglia is strongly attenuated in the absence of CCL2 (Fig. 4G) but this effect does not become apparent until the two month time point used in the present study, long after the acute elevations in CCL2 have resolved. The chain of events that occur between the peak

expression of CCL2 at 6 hrs after irradiation and the delayed quieting of microglia and recovery of neurogenesis in the second month following irradiation are unclear but are consistent with previous findings showing improved recovery one month after closed head injury in CCL2-deficient mice (with no differences in acutely measured lesion volumes and cell death after injury). The slow, improved recovery in $CCL2^{-/-}$ animals coincided with reduced macrophage infiltration, reduced neuronal loss and decreased astrocyte activation (Hughes et al., 2002; Semple et al., 2010).

We and others have shown that the proliferative population of neural stem and progenitor cells within the hippocampus is reduced by ~50% following a single dose of ionizing irradiation and the proliferative pool remains depleted for at least two-months, the longest time point evaluated in the present study (Fig 3). The absence of CCL2 has no effect on this reduction in neural progenitor proliferation, which is consistent with previous studies showing that CCL2 does not affect neural progenitor cell proliferation and cell survival (Liu et al., 2007). Rather, it appears that CCL2 plays an important role in neuronal differentiation. In CCL2 null irradiated animals, a near-normal fraction of progenitor cells that survive irradiation generate neurons (Fig. 3D,E), and maturation and arborization is increased.

The CCL2 receptor, CCR2 (a pertussis toxin-sensitive heterotrimeric G-protein-coupled receptor) is expressed by virtually all cell types in the CNS (Banisadr et al., 2002), including neural progenitor cells (Ji et al., 2004), astrocytes (Andjelkovic et al., 1999), and endothelial cells (Stamatovic et al., 2003; Thibeault et al., 2001). *In vitro* studies have shown that CCL2 directly promotes neuronal precursor cell differentiation (Edman et al., 2008; Liu et al., 2007; Turbic et al., 2011), suggesting that high levels of CCL2 might promote neurogenesis *in vivo*. In our studies, we emphasize that CCL2 is only transiently elevated in the acute phase of the irradiation response. Later, when neurogenesis has recovered, there is no evidence of CCL2/MCP-1 expression and we propose that CCL2 plays a brief instructive role in altering the neurogenic niche. This is consistent with a recent study showing that increased levels of CCL2 and CCL11 during aging are associated with decreased neurogenesis *in vivo* (Villeda et al., 2011).

With such wide spread expression of the CCL2 and its receptors, it will be difficult to identify the specific cellular targets of CCL2 in relationship to neurogenesis in the post-irradiation hippocampus. In fact, given the broad role of CCL2 in modulating both early and late inflammatory processes, it seems highly unlikely in the irradiation model that only a single cell type would be responsible for the CCL2-mediated effects. Fortunately, it may not be necessary to fully understand how CCL2 mediates its effects in order to take clinical advantage of the current observations. Biological and small molecule CCR2 antagonists are increasingly entering the clinical arena for a broad range of non-CNS inflammatory or cancer indications. It seems likely that one or more of these molecules may promote the normalization of progenitor cell function following radiation therapy. To date, these molecules have not been available for testing in our mouse model system so we are unable to confirm this interesting possibility but we are hopeful that CCL2 antagonists can be added to a growing arsenal of agents that attenuate cognitive decline following therapeutic irradiation or other forms of CNS injury or disease that are accompanied by inflammatory disruption of neurogenesis.

Supplementary Material

Refer to Web version on PubMed Central for supplementary material.

Acknowledgments

We would like to thank B. J. Rollins and E. Mocarski for their kindness in supplying CCL2 deficient animals for this work. This work was supported by grants to TDP from the Kinetics Foundation, the NIH (R01 NS045113-02, R01 MH071472) and the California Institute of Regenerative Medicine (RC1-00134). This work was also supported by an F30 NS04696701 5 to MLM; T32 GM0076365 to BJC, a National Science Foundation Graduate Research Fellowship 2004016504 to SWL and Swiss National Science Foundation, PBBEB-104450, Swiss Foundation for Medical Research grant SSMBS-1194/PASMA-108940/1 to RG, and DFG TRR43/A7 and FOR1336/B3 to JP.

References

Abayomi OK. Pathogenesis of irradiation-induced cognitive dysfunction. Acta Oncol. 1996; 35:659–663. [PubMed: 8938210]

Andjelkovic AV, Kerkovich D, Shanley J, Pulliam L, Pachter JS. Expression of binding sites for beta chemokines on human astrocytes. Glia. 1999; 28:225–235. [PubMed: 10559781]

Banisadr G, Queraud-Lesaux F, Boutterin MC, Pelaprat D, Zalc B, Rostene W, Haour F, Parsadaniantz SM. Distribution, cellular localization and functional role of CCR2 chemokine receptors in adult rat brain. J Neurochem. 2002; 81:257–269. [PubMed: 12064472]

Biswas SK, Sodhi A. In vitro activation of murine peritoneal macrophages by monocyte chemoattractant protein-1: upregulation of CD11b, production of proinflammatory cytokines, and the signal transduction pathway. J Interferon Cytokine Res. 2002; 22:527–538. [PubMed: 12060491]

Bottazzi B, Walter S, Govoni D, Colotta F, Mantovani A. Monocyte chemotactic cytokine gene transfer modulates macrophage infiltration, growth, and susceptibility to IL-2 therapy of a murine melanoma. J Immunol. 1992; 148:1280–1285. [PubMed: 1737940]

Bu J, Akhtar N, Nishiyama A. Transient expression of the NG2 proteoglycan by a subpopulation of activated macrophages in an excitotoxic hippocampal lesion. Glia. 2001; 34:296–310. [PubMed: 11360302]

Butovsky O, Ziv Y, Schwartz A, Landa G, Talpalar AE, Pluchino S, Martino G, Schwartz M. Microglia activated by IL-4 or IFN-gamma differentially induce neurogenesis and oligodendrogenesis from adult stem/progenitor cells. Mol Cell Neurosci. 2006; 31:149–160. [PubMed: 16297637]

Cameron HA, Tanapat P, Gould E. Adrenal steroids and N-methyl-D-aspartate receptor activation regulate neurogenesis in the dentate gyrus of adult rats through a common pathway. Neuroscience. 1998; 82:349–354. [PubMed: 9466447]

Chen Y, Hallenbeck JM, Ruetzler C, Bol D, Thomas K, Berman NE, Vogel SN. Overexpression of monocyte chemoattractant protein 1 in the brain exacerbates ischemic brain injury and is associated with recruitment of inflammatory cells. J Cereb Blood Flow Metab. 2003; 23:748–755. [PubMed: 12796723]

Edman LC, Mira H, Erices A, Malmersjo S, Andersson E, Uhlen P, Arenas E. Alpha-chemokines regulate proliferation, neurogenesis, and dopaminergic differentiation of ventral midbrain precursors and neurospheres. Stem Cells. 2008; 26:1891–1900. [PubMed: 18436867]

Ekdahl CT, Claasen JH, Bonde S, Kokaia Z, Lindvall O. Inflammation is detrimental for neurogenesis in adult brain. Proc Natl Acad Sci USA. 2003; 100:13632–13637. [PubMed: 14581618]

Ferreira AM, Rollins BJ, Faunce DE, Burns AL, Zhu X, Dipietro LA. The effect of MCP-1 depletion on chemokine and chemokine-related gene expression: evidence for a complex network in acute inflammation. Cytokine. 2005; 30:64–71. [PubMed: 15804597]

Filippov V, Kronenberg G, Pivneva T, Reuter K, Steiner B, Wang LP, Yamaguchi M, Kettenmann H, Kempermann G. Subpopulation of nestin-expressing progenitor cells in the adult murine hippocampus shows electrophysiological and morphological characteristics of astrocytes. Mol Cell Neurosci. 2003; 23:373–382. [PubMed: 12837622]

Ford AL, Goodsall AL, Hickey WF, Sedgwick JD. Normal adult ramified microglia separated from other central nervous system macrophages by flow cytometric sorting. Phenotypic differences defined and direct ex vivo antigen presentation to myelin basic protein-reactive CD4+ T cells compared. J Immunol. 1995; 154:4309–4321. [PubMed: 7722289]

Francis F, Koulakoff A, Boucher D, Chafey P, Schaar B, Vinet MC, Friocourt G, McDonnell N, Reiner O, Kahn A, McConnell SK, Berwald-Netter Y, Denoulet P, Chelly J. Doublecortin is a developmentally regulated, microtubule-associated protein expressed in migrating and differentiating neurons. Neuron. 1999; 23:247–256. [PubMed: 10399932]

Gage FH, Kempermann G, Palmer TD, Peterson DA, Ray J. Multipotent progenitor cells in the adult dentate gyrus. J Neurobiol. 1998; 36:249–266. [PubMed: 9712308]

Gould E, Cameron HA, Daniels DC, Woolley CS, McEwen BS. Adrenal hormones suppress cell division in the adult rat dentate gyrus. J Neurosci. 1992; 12:3642–3650. [PubMed: 1527603]

Gu L, Okada Y, Clinton SK, Gerard C, Sukhova GK, Libby P, Rollins BJ. Absence of monocyte chemoattractant protein-1 reduces atherosclerosis in low density lipoprotein receptor-deficient mice. Mol Cell. 1998; 2:275–281. [PubMed: 9734366]

Gu L, Tseng S, Horner RM, Tam C, Loda M, Rollins BJ. Control of TH2 polarization by the chemokine monocyte chemoattractant protein-1. Nature. 2000; 404:407–411. [PubMed: 10746730]

Hayashi M, Luo Y, Laning J, Strieter RM, Dorf ME. Production and function of monocyte chemoattractant protein-1 and other beta-chemokines in murine glial cells. J Neuroimmunol. 1995; 60:143–150. [PubMed: 7642742]

Hughes PM, Allegrini PR, Rudin M, Perry VH, Mir AK, Wiessner C. Monocyte chemoattractant protein-1 deficiency is protective in a murine stroke model. J Cereb Blood Flow Metab. 2002; 22:308–317. [PubMed: 11891436]

Imai Y, Ibata I, Ito D, Ohsawa K, Kohsaka S. A novel gene iba1 in the major histocompatibility complex class III region encoding an EF hand protein expressed in a monocytic lineage. Biochem Biophys Res Commun. 1996; 224:855–862. [PubMed: 8713135]

Ji JF, He BP, Dheen ST, Tay SS. Expression of chemokine receptors CXCR4, CCR2, CCR5 and CX3CR1 in neural progenitor cells isolated from the subventricular zone of the adult rat brain. Neurosci Lett. 2004; 355:236–240. [PubMed: 14732474]

Jones LL, Yamaguchi Y, Stallcup WB, Tuszynski MH. NG2 is a major chondroitin sulfate proteoglycan produced after spinal cord injury and is expressed by macrophages and oligodendrocyte progenitors. J Neurosci. 2002; 22:2792–2803. [PubMed: 11923444]

Kalm M, Fukuda A, Fukuda H, Ohrfelt A, Lannering B, Bjork-Eriksson T, Blennow K, Marky I, Blomgren K. Transient inflammation in neurogenic regions after irradiation of the developing brain. Radiat Res. 2009; 171:66–76. [PubMed: 19138045]

Kronenberg G, Wang LP, Synowitz M, Gertz K, Katchanov J, Glass R, Harms C, Kempermann G, Kettenmann H, Endres M. Nestin-expressing cells divide and adopt a complex electrophysiologic phenotype after transient brain ischemia. J Cereb Blood Flow Metab. 2005; 25:1613–1624. [PubMed: 15959463]

Lee WH, Sonntag WE, Mitschelen M, Yan H, Lee YW. Irradiation induces regionally specific alterations in pro-inflammatory environments in rat brain. Int J Radiat Biol. 2010; 86:132–144. [PubMed: 20148699]

Limoli CL, Giedzinski E, Rola R, Otsuka S, Palmer TD, Fike JR. Radiation response of neural precursor cells: linking cellular sensitivity to cell cycle checkpoints, apoptosis and oxidative stress. Radiat Res. 2004; 161:17–27. [PubMed: 14680400]

Liu XS, Zhang ZG, Zhang RL, Gregg SR, Wang L, Yier T, Chopp M. Chemokine ligand 2 (CCL2) induces migration and differentiation of subventricular zone cells after stroke. J Neurosci Res. 2007; 85:2120–2125. [PubMed: 17510981]

Lu B, Rutledge BJ, Gu L, Fiorillo J, Lukacs NW, Kunkel SL, North R, Gerard C, Rollins BJ. Abnormalities in monocyte recruitment and cytokine expression in monocyte chemoattractant protein 1-deficient mice. J Exp Med. 1998; 187:601–608. [PubMed: 9463410]

Luo Y, Laning J, Hayashi M, Hancock PR, Rollins B, Dorf ME. Serologic analysis of the mouse beta chemokine JE/monocyte chemoattractant protein-1. J Immunol. 1994; 153:3708–3716. [PubMed: 7523503]

Madsen TM, Kristjansen PE, Bolwig TG, Wortwein G. Arrested neuronal proliferation and impaired hippocampal function following fractionated brain irradiation in the adult rat. Neuroscience. 2003; 119:635–642. [PubMed: 12809684]

Matsushima K, Larsen CG, DuBois GC, Oppenheim JJ. Purification and characterization of a novel monocyte chemotactic and activating factor produced by a human myelomonocytic cell line. J Exp Med. 1989; 169:1485–1490. [PubMed: 2926331]

Mildner A, Schmidt H, Nitsche M, Merkler D, Hanisch UK, Mack M, Heikenwalder M, Bruck W, Priller J, Prinz M. Microglia in the adult brain arise from Ly-6ChiCCR2+ monocytes only under defined host conditions. Nat Neurosci. 2007; 10:1544–1553. [PubMed: 18026096]

Mizumatsu S, Monje ML, Morhardt DR, Rola R, Palmer TD, Fike JR. Extreme sensitivity of adult neurogenesis to low doses of X-irradiation. Cancer Res. 2003; 63:4021–4027. [PubMed: 12874001]

Monje ML, Mizumatsu S, Fike JR, Palmer TD. Irradiation induces neural precursor-cell dysfunction. Nat Med. 2002; 8:955–962. [PubMed: 12161748]

Monje ML, Palmer T. Radiation injury and neurogenesis. Curr Opin Neurol. 2003; 16:129–134. [PubMed: 12644738]

Monje ML, Toda H, Palmer TD. Inflammatory blockade restores adult hippocampal neurogenesis. Science. 2003; 302:1760–1765. [PubMed: 14615545]

Monje ML, Vogel H, Masek M, Ligon KL, Fisher PG, Palmer TD. Impaired human hippocampal neurogenesis after treatment for central nervous system malignancies. Ann Neurol. 2007; 62:515–520. [PubMed: 17786983]

Muessel MJ, Klein RM, Wilson AM, Berman NE. Ablation of the chemokine monocyte chemoattractant protein-1 delays retrograde neuronal degeneration, attenuates microglial activation, and alters expression of cell death molecules. Brain Res Mol Brain Res. 2002; 103:12–27. [PubMed: 12106688]

Ogata H, Takeya M, Yoshimura T, Takagi K, Takahashi K. The role of monocyte chemoattractant protein-1 (MCP-1) in the pathogenesis of collagen-induced arthritis in rats. J Pathol. 1997; 182:106–114. [PubMed: 9227349]

Okabe M, Ikawa M, Kominami K, Nakanishi T, Nishimune Y. 'Green mice' as a source of ubiquitous green cells. FEBS Lett. 1997; 407:313–319. [PubMed: 9175875]

Pais TF, Chatterjee S. Brain macrophage activation in murine cerebral malaria precedes accumulation of leukocytes and CD8+ T cell proliferation. J Neuroimmunol. 2005; 163:73–83. [PubMed: 15885309]

Palmer TD, Willhoite AR, Gage FH. Vascular niche for adult hippocampal neurogenesis. J Comp Neurol. 2000; 425:479–494. [PubMed: 10975875]

Priller J, Flugel A, Wehner T, Boentert M, Haas CA, Prinz M, Fernandez-Klett F, Prass K, Bechmann I, de Boer BA, Frotscher M, Kreutzberg GW, Persons DA, Dirnagl U. Targeting gene-modified hematopoietic cells to the central nervous system: use of green fluorescent protein uncovers microglial engraftment. Nat Med. 2001; 7:1356–1361. [PubMed: 11726978]

Ramprasad MP, Terpstra V, Kondratenko N, Quehenberger O, Steinberg D. Cell surface expression of mouse macrosialin and human CD68 and their role as macrophage receptors for oxidized low density lipoprotein. Proc Natl Acad Sci USA. 1996; 93:14833–14838. [PubMed: 8962141]

Saxe MD, Battaglia F, Wang JW, Malleret G, David DJ, Monckton JE, Garcia AD, Sofroniew MV, Kandel ER, Santarelli L, Hen R, Drew MR. Ablation of hippocampal neurogenesis impairs contextual fear conditioning and synaptic plasticity in the dentate gyrus. Proc Natl Acad Sci U S A. 2006; 103:17501–17506. [PubMed: 17088541]

Semple BD, Kossmann T, Morganti-Kossmann MC. Role of chemokines in CNS health and pathology: a focus on the CCL2/CCR2 and CXCL8/CXCR2 networks. J Cereb Blood Flow Metab. 2010; 30:459–473. [PubMed: 19904283]

Shors TJ, Miesegaes G, Beylin A, Zhao M, Rydel T, Gould E. Neurogenesis in the adult is involved in the formation of trace memories. Nature. 2001; 410:372–376. [PubMed: 11268214]

Shors TJ, Townsend DA, Zhao M, Kozorovitskiy Y, Gould E. Neurogenesis may relate to some but not all types of hippocampal-dependent learning. Hippocampus. 2002; 12:578–584. [PubMed: 12440573]

Stamatovic SM, Keep RF, Kunkel SL, Andjelkovic AV. Potential role of MCP-1 in endothelial cell tight junction 'opening': signaling via Rho and Rho kinase. J Cell Sci. 2003; 116:4615–4628. [PubMed: 14576355]

Thibeault I, Laflamme N, Rivest S. Regulation of the gene encoding the monocyte chemoattractant protein 1 (MCP-1) in the mouse and rat brain in response to circulating LPS and proinflammatory cytokines. J Comp Neurol. 2001; 434:461–477. [PubMed: 11343293]

Traynor TR, Herring AC, Dorf ME, Kuziel WA, Toews GB, Huffnagle GB. Differential roles of CC chemokine ligand 2/monocyte chemotactic protein-1 and CCR2 in the development of T1 immunity. J Immunol. 2002; 168:4659–4666. [PubMed: 11971015]

Turbic A, Leong SY, Turnley AM. Chemokines and inflammatory mediators interact to regulate adult murine neural precursor cell proliferation, survival and differentiation. PLoS One. 2011; 6:e25406. [PubMed: 21966521]

van Praag H, Schinder AF, Christie BR, Toni N, Palmer TD, Gage FH. Functional neurogenesis in the adult hippocampus. Nature. 2002; 415:1030–1034. [PubMed: 11875571]

Vela JM, Yanez A, Gonzalez B, Castellano B. Time course of proliferation and elimination of microglia/macrophages in different neurodegenerative conditions. J Neurotrauma. 2002; 19:1503–1520. [PubMed: 12490014]

Villeda SA, Luo J, Mosher KI, Zou B, Britschgi M, Bieri G, Stan TM, Fainberg N, Ding Z, Eggel A, Lucin KM, Czirr E, Park JS, Couillard-Despres S, Aigner L, Li G, Peskind ER, Kaye JA, Quinn JF, Galasko DR, Xie XS, Rando TA, Wyss-Coray T. The ageing systemic milieu negatively regulates neurogenesis and cognitive function. Nature. 2011; 477:90–94. [PubMed: 21886162]

Weissleder R, Elizondo G, Wittenberg J, Lee AS, Josephson L, Brady TJ. Ultrasmall superparamagnetic iron oxide: an intravenous contrast agent for assessing lymph nodes with MR imaging. Radiology. 1990; 175:494–498. [PubMed: 2326475]

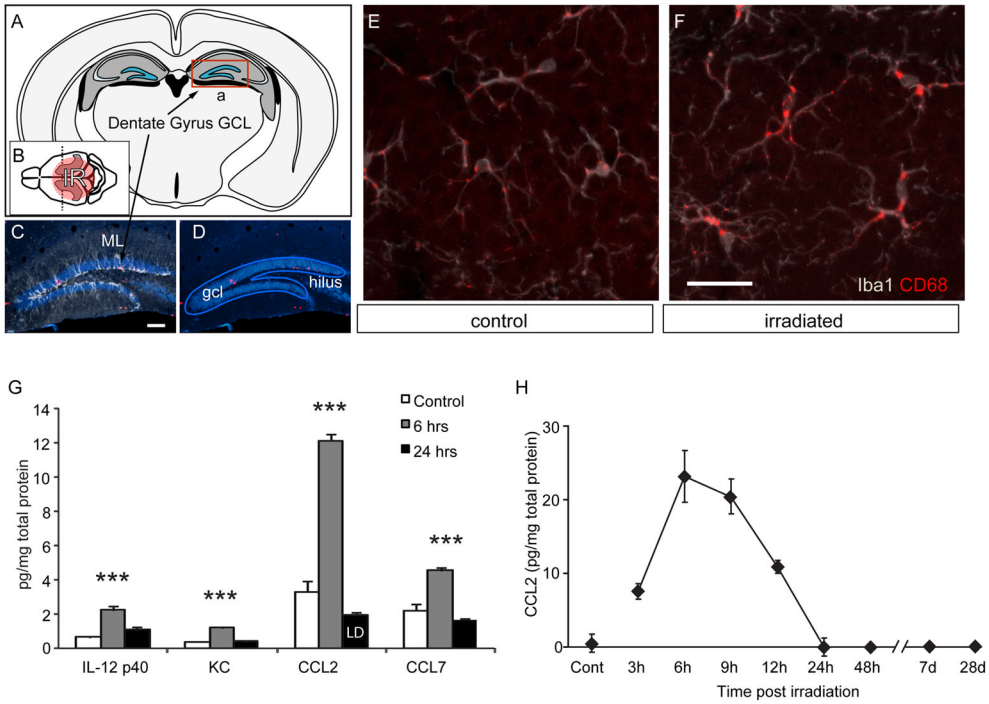

Figure 1. Microglial activation and chemokine expression in the hippocampal formation following cranial irradiation

A Coronal schematic of the adult mouse brain shows the location of the hippocampal formation (grey) and dentate granule cell layer (blue) where neurogenesis continues throughout adult life. **B** A sagittal view shows the circular column of tissues (red) exposed to 10 Gy of ionizing X-irradiation (IR) **C,D** Mature neurons within the granule cell layer (GCL) of the dentate gyrus are brightly stained by NeuN (blue). Neural progenitor cells divide at the boundary between the GCL and hilus to form a dense band of doublecortin-positive immature neurons (white) that arborize extensively within molecular layer (ML). **E, F** Iba1-positive microglia (white) within the neurogenic zone of the GCL become activated following irradiation and become strongly positive for the activation marker CD68 (red), a lysosome-associated epitope that is upregulated in activated macrophages and microglia. **G** Luminex assays were used to evaluate cytokine and chemokine abundance in hippocampal tissue extracts at 6 and 24 hrs after irradiation. Of 23 proteins assayed, only 4 were elevated above background following irradiation but each returns to normal levels within 48 hrs (LD = value at limits of detection). ANOVA posthoc Newman-Keuls, IL-12 p40, $F(2,9) = 27.01$, $p<0.001$; KC, $F(2,9) = 110.2$, $p<0.001$; CCL2, $F(2,9) = 177.8$, $p<0.001$, CCL7, $F(2,9) = 36.86$, $p<0.001$. *** $p < 0.001$. **H** CCL2 protein levels measured by ELISA peak at 6, return to normal levels within 24 hrs, and remain undetectable above background in the following weeks.

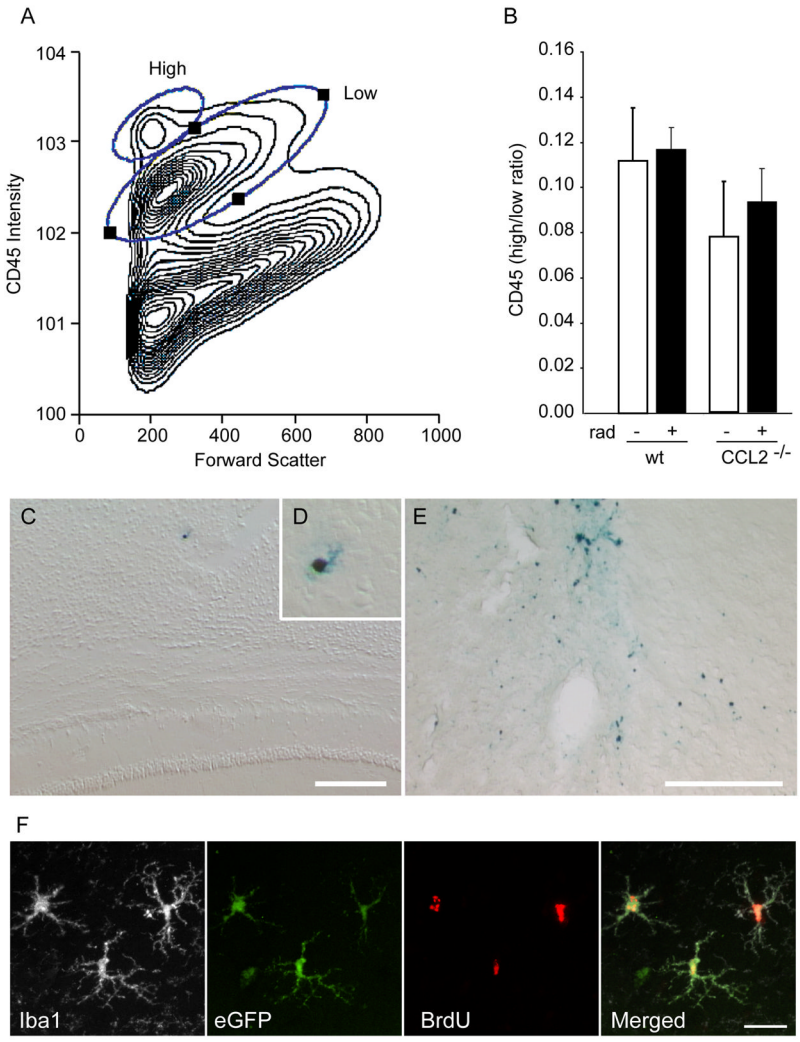

Figure 2. CCL2 acts on resident cells rather than through recruitment of peripheral monocytes

A, B, Flowcytometric analysis of CD45 intensity within cells isolated from control and irradiated brains one week after irradiation. Staining intensity and forward scatter for a representative total cell prep is shown in the contour plot in A. This data was then gated on CD11b (monocyte-specific) staining and the ratio of CD45 high vs. low monocytes calculated in B. The results show that there is no radiation-induced increase in the relative abundance of CD45-high vs. low monocytes present within the brains of either WT or $CCL2^{-/-}$ animals. **C, D, E** Prussian blue staining for the presence of iron-labeled macrophages revealed the exceedingly rare cell in the irradiated brain (C, D). In contrast, abundant iron-labeled peripheral macrophages are present in control brains one week following a focal ischemic stroke (E). A single blue stained macrophage can be seen in the cortex overlying the hippocampus of a WT irradiated mouse brain (C and higher magnification in D). There were no iron-labeled microglia detected within the hippocampal formation of any animal. In contrast to irradiation, an area of rat brain adjacent to a cortical focal ischemic injury shows significant recruitment of iron-labeled peripheral macrophages (E). **F** Animals that received eGFP-expressing bone marrow transplants concurrent with cranial irradiation showed very few GFP-positive cells in the hippocampus. In irradiated brains, some of these cells were ramified and located in the brain parenchyma, whereas only perivascular cells were found in non-irradiated brains. This confirms that peripheral

monocyte recruitment was negligible compared with the activation of resident microglia in this radiation injury model.

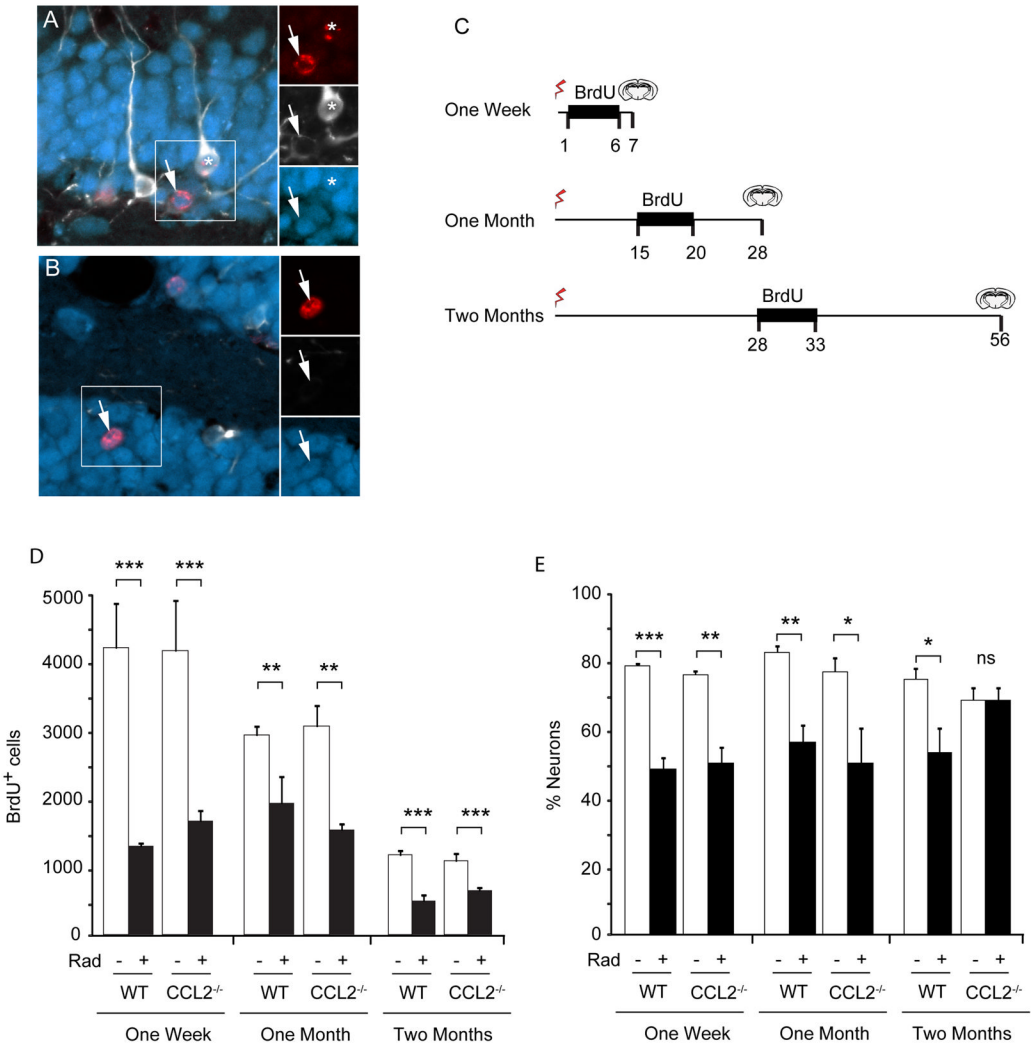

Figure 3. Impact of irradiation on neurogenesis in WT and CCL2$^{-/-}$ mice

A, B Newborn cells within the dentate gyrus are labeled with BrdU (red). Initially newborn neurons express doublecortin (white) and then express NeuN (blue) as they begin to mature. The total population of newborn neurons includes immature neurons that express Dcx alone, cells that are in transition and express both Dcx and NeuN (asterisk in A), as well as more mature neurons that lose Dcx expression and become predominantly NeuN-positive (arrows in A, B). **C** Three BrdU labeling paradigms were used to evaluate neurogenesis at different times following irradiation. BrdU was injected daily during the indicated interval to label dividing cells and tissue then taken at the indicated times and evaluated for neurogenesis. **D** The total number of BrdU positive cells was determined within the GCL. Irradiation caused a significant depletion of dividing cells in both wild type (WT) and CCL2−/− animals at all time points. ANOVA revealed significant treatment effect, 1 week, $F(3,12) = 12.72$, $p<0.001$; 1 month, $F(3,12) = 9.819$, $p<0.01$; 2 month $F(3,32) = 13.87$, $p<0.001$. Posthoc Newman-Keuls test, $^{**}p < 0.01$, $^{***}p < 0.001$. **E** The fraction of newborn neurons (cells that expressed BrdU and neuronal markers Dcx and/or NeuN) was reduced 1 week and 1 month after irradiation, but gradually recovered in CCL2$^{-/-}$ animals two month after irradiation. ANOVA, overall treatment effect, 1 week, $F(3,12) = 39.85$, $p<0.001$; 1 month, $F(3,12) = 8.471$, $p<0.01$; 2 month $F(3,32) = 4.363$, $p<0.05$. Posthoc Newman-Keuls, * $p<0.05$, $^{**}p<0.01$, $^{***}p<0.001$, ns, not significant.

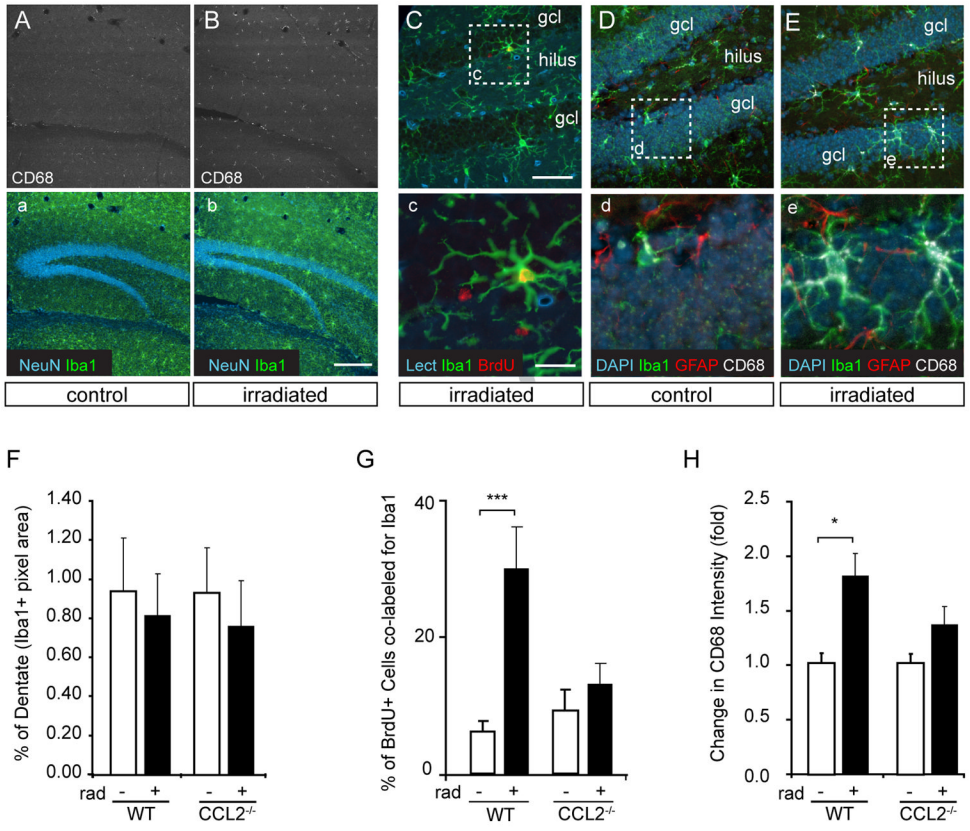

Figure 4. Absence of CCL2 attenuates radiation-induced microglial proliferation and activation

A, B, Low magnification images of control vs. irradiated wild type hippocampus show a persistent increase in CD68 staining in wild type animals two months after the initial 10 Gy dose. **C** Irradiation (rad) is accompanied by chronic proliferation of microglia in wild type (WT) animals but not in $CCL2^{-/-}$ animals. The confocal micrograph in C shows Iba1 positive microglia (green) adjacent to the granule cell layer (gcl) in an irradiated WT animal. Many microglia are still proliferative and become BrdU labeled (red) one month after a single 10 Gy dose of X-irradiation. The vascular profiles are stained with tomato lectin (Lect, blue). Boxed area in C is shown at higher magnification in c. **D, E,** Microglia in control vs. irradiated WT animals are shown in D and E respectively. CD68 staining (white), a marker for microglial activation, is more abundant in WT animals following irradiation (E, e). Astrocyte processes are shown in red (GFAP) and cell nuclei are shown in blue (DAPI). Boxed areas of D and E are shown at higher magnification in d and e, respectively. **F** Quantification of Iba1+ pixels within the dentate gyrus shows no change in the relative abundance or arborization of microglia in WT or $CCL2^{-/-}$ animals two months after irradiation (see also Supplemental Fig. 1). **G, H** In contrast, the mitotic activity and intensity of CD68 staining on microglia increased in WT but not $CCL2^{-/-}$ animals following irradiation suggesting that the absence of CCL2 attenuated microglial proliferation and activation. ANOVA posthoc Newman-Keuls, BrdU+Iba1+, $F(3,32) = 10.77$, ***$p<0.001$; CD68, $F(3,32) = 3.167$, *$p<0.05$.

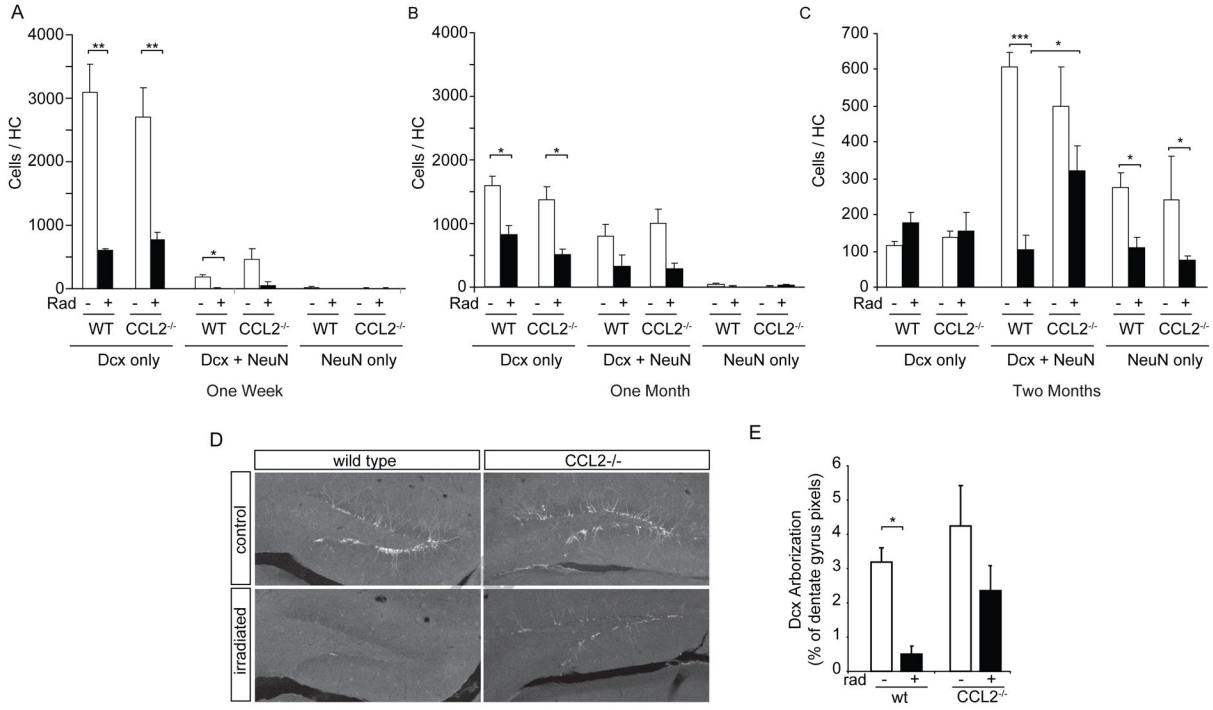

Figure 5. Impaired neuronal maturation following irradiation is partially reversed in CCL2$^{-/-}$ animals

A–C Confocal evaluation of BrdU-labeled neurons for expression of Dcx and/or NeuN at one week, one month and two months after irradiation (see Fig. 3 for BrdU labeling paradigms). The abundance of immature (Dcx only), transition state (Dcx+NeuN) or mature (NeuN only) neurons was strongly reduced in both WT and CCL2$^{-/-}$ animals at one week (**A**) and one month (**B**) following irradiation. Two-way ANOVA, treatment effect, 1 week, $F(3,27) = 19.92$, $p<0.001$; 1 month, $F(3,33) = 13.87$, $p<0.001$; posthoc Bonferroni, $^{**}p < 0.01$, $^{*}p < 0.05$. (**C**) Cells evaluated at two months following irradiation show that absence of CCL2 significantly increased the number of transition state neurons when comparing CCL2 irradiated versus irradiated WT animals. Two-way ANOVA, $F(3,72) = 10.79$, $p<0.001$, posthoc Bonferroni, $^{***}p < 0.001$, $^{*}p < 0.05$. **D, E** Dcx abundance (pixel area) and staining intensity shows that irradiation results in the depletion of Dcx-positive arbors within the dentate gyrus of WT animals. The absence of CCL2 attenuates this depletion. ANOVA, $F(3,32) = 7.690$, $p<0.001$, posthoc Newman-Keuls, $^{*}p < 0.05$.